Scanning Force Microscopy in Biology

A high-resolution instrument that can operate in liquids is making complex biological structures accessible to study in conditions close to those that exist in living organisms.

Carlos Bustamante and David Keller

Microscopes have played a fundamental role in the development of biology as an experimental science. It was Robert Hooke who, when using a compound microscope in 1655, noticed that thin slices of cork were made up of identical and small self-contained units, which he called "cells." The generalization of this observation and its acceptance, though, had to wait until the late 1830s, when German microscopists Matthias Schleiden and Theodor Schwann—working independently—introduced the "cell theory" of complex organisms. By the second half of the 19th century Magnus Retzius, Santiago Ramón y Cajal and Camillo Golgi were busy completing the microscopic anatomical description of the cell.

Meanwhile, in the 1870s, Ernst Abbe's diffraction theory of imaging set the theoretical resolution limits for the optical microscope and showed that it was inadequate for studying cellular fine structure. The breakthrough occured in the early 1930s, when the transmission electron microscope, built by Ernst Ruska, extended the resolution to the nanometer scale, thereby making possible the ultrastructural description of cellular architecture.

But despite its limitations, the optical microscope has remained essential to biological research because it can image samples in water, thus making it possible to observe biological processes in real time. For many years researchers have struggled to combine the high-resolution advantages of the electron microscope with the in-water operating capabilities of the optical microscope. The invention of the scanning tunneling microscope by Gerd Binnig and Heinrich Rohrer in 1981 opened a new approach to achieving this goal. The STM was the first member of a new class of instruments called scanning probe microscopes, which are all based on similar principles. (See the article by Daniel Rugar and Paul Hansma, PHYSICS TODAY, October 1990, page 23.)

Scanning probe microscopes do not use lenses to form images. Instead, they use a sharply pointed sensor tip to detect some property of the sample surface. The main difference between one type of probe microscope and another is the nature of the tip and the corresponding tip–sample interaction. Although the STM has not found extensive application in biology, another member of this class of instruments, the scanning force microscope,[1] is now emerging as a useful tool in biological research.[2]

The SFM can operate at least as well in liquid as in air, so it is possible to image biological molecules in aqueous buffers—that is, under conditions close to their native environment. The resolution in scanning force microscopy is determined by the sharpness of the tip and is typically between 5 and 10 nanometers. (See box 1 on page 35 for a general discussion of resolution in SFMs.) The SFM is therefore the first—and so far the only—microscope that can achieve nanometer-scale resolution on biological samples under native conditions. As figure 1 illustrates, this capability is already being used to follow processes of macromolecular assembly.

CARLOS BUSTAMANTE *is a Howard Hughes Medical Institute investigator, member of the Institute of Molecular Biology and professor of chemistry at the University of Oregon, in Eugene.*
DAVID KELLER *is a professor of chemistry at the University of New Mexico, in Albuquerque.*

SFM Basics

In an SFM the tip is mounted on the end of a flexible cantilever. As the sample is scanned beneath the tip, small forces of interaction with the sample cause the cantilever to deflect, revealing the sample's topography. Deflections as small as 0.01 nm can be detected. A variety of methods have been devised to detect the cantilever deflection.[3] The most common approach, called an optical lever, is to reflect a laser beam off the back side of the cantilever into a four-segment photodetector. The difference in output between the detectors is then proportional to the deflection amplitude. The optical lever is essentially a motion amplifier: The deflection of the laser spot at the photodetector is proportional to the deflection of the cantilever[3] with a gain factor, g. The value of g is typically 300–1000, so a deflection of 0.01 nm at the cantilever becomes a displacement of 3–10 nm at the photodetector, large enough to generate a measurable voltage. In fact, the limiting factor in motion detectors is not the sensitivity of the detector itself but the intrinsic vibration of the cantilever due to thermal energy.

One can operate the SFM in three different modes: contact, noncontact and tapping.

In the contact mode the tip touches the sample at all times, sliding over the surface as the sample is scanned. The contact mode usually produces stable, high-resolution images, but compression and shear forces generated between the tip and surface may cause damage. This possibility can be especially troublesome when imaging biomolecules, which are almost always soft and only

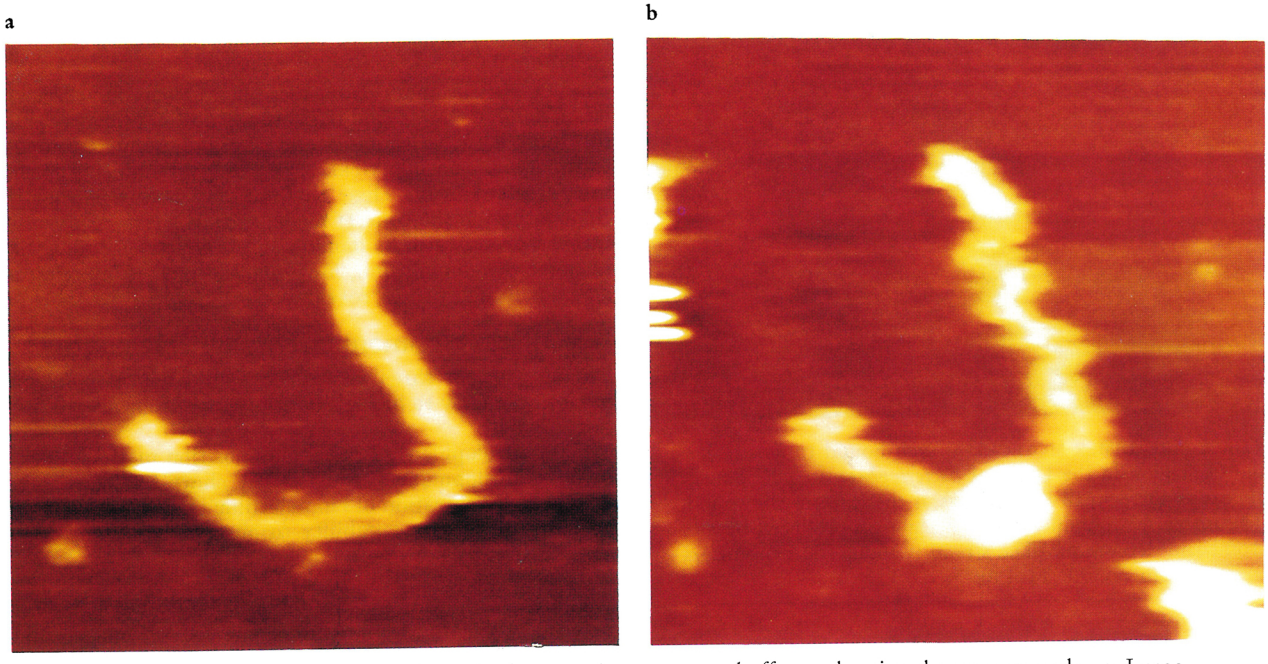

SCANNING FORCE MICROSCOPY IMAGES of a DNA fragment in an aqueous buffer made using the contact mode. **a:** Image obtained immediately after flushing the liquid cell with 300 microliters of 1 nanomolar of *Escherichia coli* RNA polymerase solution. **b:** Second scan after protein injection. A single polymerase molecule has docked on the DNA fragment. (From ref. 12, courtesy of Martin Guthold, University of Oregon.) FIGURE 1

weakly attached to the substrate.

In the noncontact mode, one oscillates the tip at high frequency (100 kilohertz to 1 megahertz) a few nanometers above the surface.[3–5] This oscillation greatly increases the sensitivity of the microscope, so that even weak, long-range forces such as attractive van der Waals forces and electrostatic forces can be detected. During scanning, the topography of the surface is tracked by following the effect of these forces on the amplitude, phase or frequency of the cantilever oscillation.[5] It is therefore possible to image even the softest samples without damage. In practice the noncontact mode is difficult to use because the tip is easily captured by adhesive forces at the surface. Also, the resolution is usually lower than in the contact mode, because of the relatively large tip–sample distance. (See box 3 on page 38.) So far, the noncontact approach has not been routinely adapted for imaging in liquids, and little information exists on biological applications.

In the tapping mode the cantilever is also oscillated, but with a larger amplitude, and the tip is allowed to make transient contact with the sample at the bottom of its swing. The tapping mode is a compromise between the contact and noncontact modes: Because the tip makes contact with the sample, the resolution is usually almost as good as in contact mode, but because the contact is very brief, the damage caused by shear forces is almost completely eliminated. Also, the tapping mode recently has been adapted for imaging in liquids, and its application to biological molecules in aqueous environments is increasing rapidly. (See reference 6 for a recent review.)

Tip–sample interactions

A large number of forces act simultaneously between the tip and the sample in any SFM experiment. Their effect on the image depends on the size of the dominant forces, the SFM's mode of operation, the environment of the tip, the properties of the sample and the sharpness and shape of the tip.

In the contact and tapping modes in air, where the tip is close to the sample surface, capillary forces and atomic repulsions between the tip and the sample are dominant. All samples have a thin layer of water on their

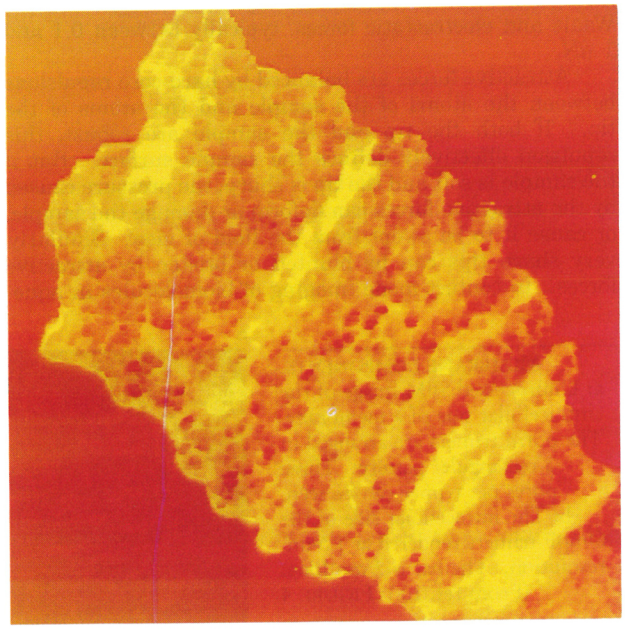

CONTACT-MODE IMAGE of a polytene chromosome from the salivary gland of the common fruit fly, obtained in air using a tip produced by electron-beam deposition. The width of the chromosome is about 6 microns. (From ref. 8, courtesy of Eric Henderson, Iowa State University.) FIGURE 2

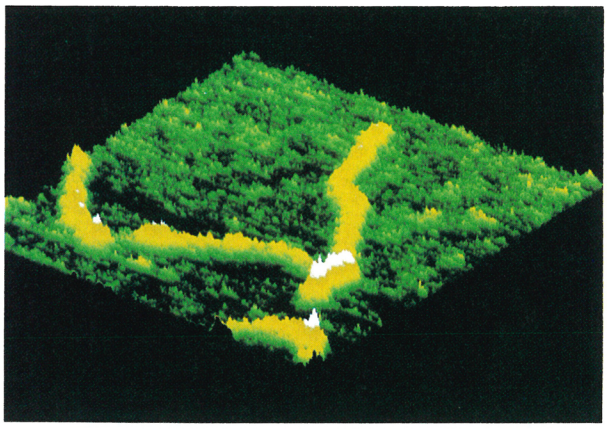

THREE CRO DIMER MOLECULES, each bound to its site at the O_R region in the DNA of *bacteriophage* λ. The dimers appear as three small light domes at the kink in the strand. The image was obtained in air using a tip produced by electron-beam deposition. The strand is about 200 nanometers long. (From ref. 9.) FIGURE 3

surfaces in ambient air. Even a few monolayers of adsorbed water can generate an attractive capillary force as large as a few hundred nanonewtons.[2,7] (This force can be reduced to about 10 nN by decreasing the ambient humidity.) In the contact mode the capillary force pins the tip to the surface and puts a limit on the lowest stable imaging force, and hence on the minimum tip and sample damage. In the tapping mode it puts a lower limit on the amplitude of oscillation required to prevent capture of the tip. In the noncontact mode the capillary force often prevents imaging altogether.

One way around this problem is to eliminate the liquid–air interface by imaging in liquids. Tip–sample interactions are then dominated by much smaller van der Waals and electrostatic forces, typically between 0.1 and 1 nN.

Attractive forces are balanced by hard-core repulsions between the atoms of the sample and the atoms of the tip. If both the tip and the sample are robust, this repulsion effectively defines the sample surface. But if the sample is soft and the tip is sharp, the pressure caused by the attractive forces can deform or damage the sample, or cause it to be swept from the field of view. Similarly, very sharp tips can be blunted or broken by attractive forces. In contact-mode imaging of biomolecules in aqueous buffers, the main experimental problems are damage being done to the tip and the sample, and the tip sweeping the sample away. Tapping-mode imaging reduces damage to the sample in many cases, probably by reducing shear forces, but it is not clear that tapping is any gentler to the tip than is the contact mode, so that sharp, high-resolution tips may still be damaged in practice. For all these reasons, developing new, low-force methods of imaging is a major focus of SFM research.

Recent developments in biological imaging

During the last three years, the application of scanning force microscopy to biology has benefited from progress in four areas:

▷ The development of reliable deposition methods.
▷ The development of consistently sharp tips.
▷ The demonstration of biomolecular imaging in aqueous buffers and of the capability to observe molecular processes in aqueous buffers.
▷ The development of the tapping mode in liquids.

We illustrate here some recent applications of biological imaging in air and liquids, using the contact and tapping modes.

Contact-mode imaging in air. Figure 2 shows a contact-mode image in air of a polytene chromosome from the salivary gland of the common fruit fly, *Drosophila melanogaster*.[8] These chromosomes have a characteristic pattern of dense bands and loosely condensed regions called interbands. The interbands correspond to regions of high transcriptional activity. (Transcription is the copying of the DNA into a messenger RNA molecule by an RNA polymerase protein.) The image in figure 2 was obtained with a high-aspect-ratio tip fabricated by electron-beam deposition techniques.[2] Generally, sharper tips lead to higher resolution and depth discrimination but may also cause sample damage, as discussed in box 2 on page 36.

Tapping-mode imaging in air. Figure 3 depicts a tapping-mode image in air of three pairs of Cro molecules bound to three adjacent sites—called operator sites—in DNA.[9] Cro, a protein from a virus known as *bacteriophage* λ, binds as a dimer (two Cro molecules together) to each operator site. The three peaks correspond to three Cro dimers. The competition of Cro molecules with another protein, the λ repressor, for these same sites constitutes a genetic switch that regulates the transcriptional activity in *bacteriophage* λ.

With a molecular weight of only 14.7 kilodaltons (1

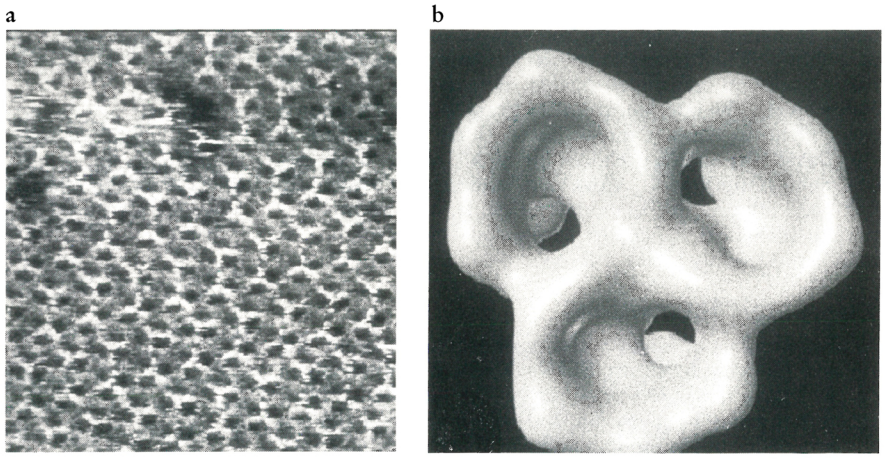

MEMBRANE COMPONENTS. **a:** Unprocessed SFM image of the intracellular side of a membrane. The porin trimers are arranged in a rectangular pattern. Three pores per trimer can be seen. **b:** The intracellular side of the OmpF trimers rendered at 1.5-nm resolution. The bar is 2 nm long. (From ref. 10.) FIGURE 4

Box 1. Resolution in SFMs

At present there is no generally accepted definition of resolution in probe microscopy. Part a of the accompanying figure illustrates the reason. The sample consists of a pair of sharp spikes separated by distance d. They are imaged by a parabolic tip with end radius R. Because the sample is sharper than the tip, the image is a pair of inverted tips that appear to hang on the spikes. The intersection of these surfaces defines a small dimple between the spikes of depth Δz, which is determined by the shape and size of the tip and by the separation distance d. One definition of "resolution" is then the minimum separation d for which the dimple depth Δz is larger than the instrumental noise. This is the closest analog for SFM imaging to the Rayleigh definition of resolution in optical microscopy.

One difficulty with this simple idea is shown in part b of the figure. As the height difference between the two spikes increases, the depth of the dimple decreases so that two spikes that are resolved when their heights are nearly equal may not be resolved when their heights are unequal. This example shows that resolution in SFM, unlike in optical microscopy, is a function of the height difference between adjacent features and must be decided separately for each feature in an image. This property is a consequence of the fundamentally nonlinear nature of SFM image formation.

Using the preceding definition of resolution, the minimum separation d that will result in a dimple of depth Δz for spikes with height difference Δh imaged by a parabolic tip is given by the equation

$$d = \sqrt{2R}\left(\sqrt{\Delta z} + \sqrt{\Delta z + \Delta h}\right)$$

for $d > \sqrt{2R\Delta h}$. For features of equal height, a parabolic tip with an end radius of 10-nm and a detectable dimple depth of 0.5 nm yields a minimum resolved separation d of 6.4 nm. By comparison, if the height difference is 2.0 nm, the minimum resolved separation is 12.5 nm. The definition used above assumes strictly rigid contact surfaces. In practice the sample tends to deform under tip pressure and the actual resolution can therefore be better or worse than that predicted by the above equation, depending on the geometry of the sample and its elastic properties.

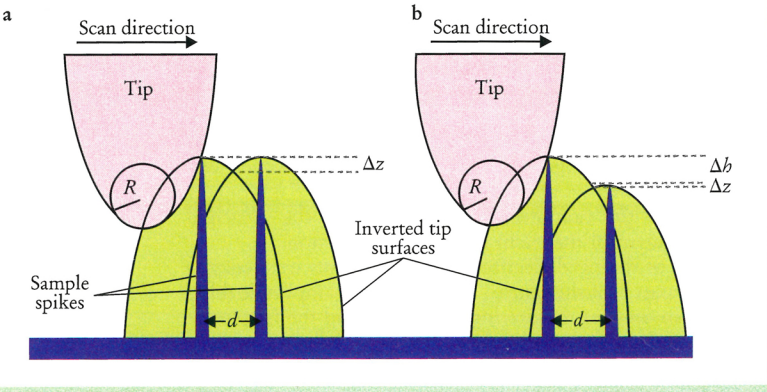

dalton = 1 atomic mass unit), these dimers are among the smallest proteins imaged by any kind of microscopy. The distance between each peak is 7.1 nm and the dimple between dimers is 0.3 nm, barely above the noise level in the image. Thus, according to the resolution criterion of the equation in box 1, the optimal resolution in this image is about 7 nm. This result indicates that the SFM can be used to characterize complex multiprotein assemblies involved in the essential processes of transcription and replication. The elucidation of the spatial relationships in these complex structures is one of the most important challenges in modern structural biology.

Contact-mode imaging in liquids. Contact-mode scanning force microscopy has been used to image DNA molecules in propanol, water and aqueous buffers.[2,6] Contact imaging in liquids has proven particularly advantageous for imaging membrane proteins in physiological environments. Figure 4a is an image of two-dimensional crystals of the intracellular side of OmpF porin imaged in buffer. This protein is a major component of the outer membrane of *Escherichia coli* and functions as a molecular sieve,[10] allowing passage of molecules of up to 600 daltons. The two-dimensional crystalline order makes increased spatial resolution and discrimination possible through the use of Fourier-based image processing methods (figure 4b). (For a recent review article see reference 11.)

Imaging in aqueous buffer solutions preserves the native structure of biomolecules, making it possible to follow, for example, the assembly of protein–DNA complexes. Figure 1 shows the binding of *E. coli* RNA polymerase to DNA in two consecutive frames obtained within two minutes after injection of a polymerase-containing solution into the sample chamber.[12] In the earliest image (figure 1a) the DNA fragment is seen before binding of the polymerase. In the next frame (figure 1b), obtained approximately one minute later, a high feature about 20 nm in diameter and identified as an RNA polymerase molecule, can be seen bound to the DNA fragment. The scanned area is 0.3 × 0.3 microns—the size of the smallest (single-color) picture element, or pixel, in an optical microscope image. This example illustrates the unique position of the SFM as a bridge between optical and electron microscopes.

Tapping-mode imaging in liquids. The tapping mode in liquids minimizes shear forces between the tip and the sample (see box 2 on page 36), thus making it possible to image molecules that are only weakly attached to the substrate. Figure 5 is a time-lapse sequence showing the digestion of a DNA fragment by Bal 31 nuclease.[6] The first image was taken just before the addition of the nuclease, and the other images were taken 12 and 24 minutes after the addition of nuclease. The nuclease is not seen because it interacts only transiently with the DNA during catalysis. As the DNA is digested, it disappears from the image, leaving increasingly large gaps in the molecule. Tapping-mode imaging in liquid eliminates the need to attach the molecules strongly to the surface, a requirement that could interfere with the molecular recognition needed in biological activity. It may therefore become the method of choice for following biochemical processes as they take place.[6,13]

Image processing and simulation

For lens-based microscopes, such as optical and electron

Box 2. The physics of tapping in liquids

In the tapping mode the oscillating tip touches the surface once each cycle. Changes in the amplitude and phase of the cantilever caused by this interaction are used to form the image. Experimentally, it is found that the amplitude of the oscillation decreases as the tip comes into contact with the sample, even though the cantilever is strongly damped by viscous friction. Part a of the accompanying figure shows a "tapping curve," in which the cantilever deflection is plotted against time as the sample is raised to interact with the tip. When the tip is far from the sample (point A), the peak-to-peak deflection is about 20 nm. As the tip begins to interact with the surface (point B), the amplitude decreases monotonically until the tip is pressed completely onto the surface (point C).

There is no well-established explanation for how the tapping mode works in liquids, but the following model appears to explain the known data. The motion of a thin elastic beam subject to viscous damping is governed by the fourth-order wave equation

$$EI\frac{\partial^4 z}{\partial s^4} + g\frac{\partial z}{\partial t} + \rho\frac{\partial^2 z}{\partial t^2} = 0$$

where $z(s,t)$ is the bending profile (the height of the bent beam at a distance s along its length), ρ is the beam's mass per unit length, g is its friction coefficient per unit length, E is Young's modulus for the cantilever material and I is the principal second moment of inertia in the bending direction.[17]

A plot of the tip deflection amplitude versus frequency is shown in part b of the figure. The deflection amplitude (blue curve) is in units of the driving amplitude, and the frequency is in units of the first corner frequency $\omega_c = k_c/\gamma$, where k_c is the cantilever force constant and γ is the effective cantilever damping constant. The black curve shows the phase difference between the cantilever deflection and the height of the tip above the sample. The red curve shows the phase difference between the cantilever deflection and the negative of the driving vibration x_0. These plots depict two important features of overdamped cantilever motion in liquids:

▷ The cantilever deflection can be larger than the amplitude of the driving vibration, despite strong damping. The tip deflection is greater than the driving vibration because the viscous forces are distributed over the length of the cantilever, and forces acting at positions back from the tip end are amplified by the wagging of the tip. The figure shows that these so-called hyperdeflections occur over a wide range of frequencies.

▷ There is a special frequency (point P) at which the cantilever deflection x_T is 180 degrees out of phase with the driving vibration v and exactly in phase with the height z_T of the tip above the sample:

$$x_T = x_0\cos\omega t,\ v = -v_0\cos\omega t,\ z_T = z_0\cos\omega t$$

At this frequency the tip reaches its minimum height (and strikes the surface) exactly when the cantilever deflection is at its negative maximum and the driving vibration is at its positive maximum. When the tip encounters the surface under these conditions, the downswing of the cantilever is halted and the bottom of the tapping curve is clipped (between points B and C in part a of the figure). The maximum force exerted on the sample during contact can then be approximated as

$$F_{max} = k_c\,\Delta x_{max}$$

where k_c is the force constant of the cantilever and Δx_{max} is the change in deflection amplitude. In a typical tapping-mode experiment, the force constant is about 0.4 newtons per meter, and the change in amplitude varies between 0.1 and 0.5 nm, so the maximum force is between 4×10^{-11} and 2×10^{-10} nN. This force is roughly an order of magnitude smaller than typical forces exerted in the contact mode. On the other hand the minimum value of F_{max} is determined by the smallest detectable value of Δx_{max}, which is ultimately limited by the thermal vibration of the cantilever.

One measure of the damage to the sample in the tapping mode is the work done during the period of contact between tip and sample:

$$w = \frac{k_c^2 x_0^2 l}{2E_s A}[1-\cos(\omega\tau/2)]^2$$

where

$$\omega\tau = 2\cos^{-1}\left(\frac{x_0-\Delta x}{x_0}\right)$$

and A is the area of the sample in contact with the tip, E_s is the Young's modulus of the sample and l is its thickness. When $\omega\tau \ll 1$:

$$w = \frac{k_c^2 x_0^2 l}{128E_s A}\omega^4\tau^4 = \frac{k_c^2 l}{2E_s A}(\Delta x)^2$$

In this limit, the energy dissipated on the sample is, as expected, independent of the total amplitude of oscillation, but depends quadratically on the change in amplitude Δx. The sharper the tip (the smaller the tip–sample contact area) and the stiffer the cantilever, the greater the damage to the sample.

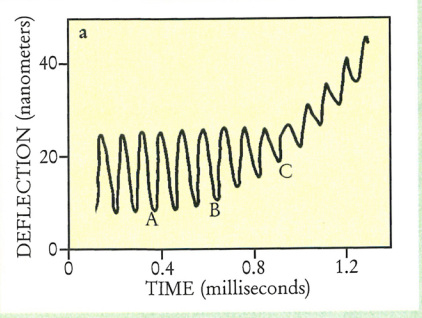

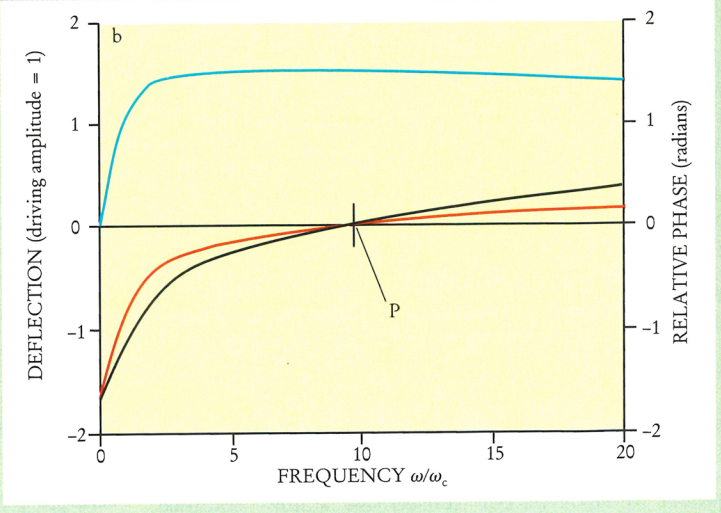

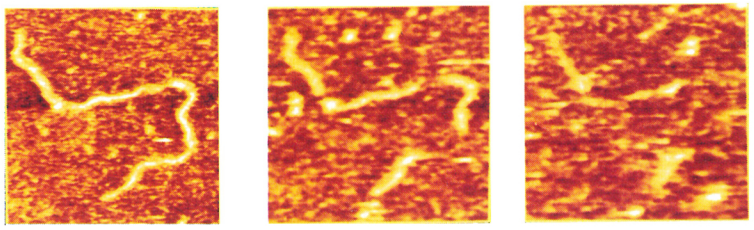

DIGESTION. The three sequential images (at 0, 12 and 24 minutes) show the digestion of a DNA fragment by Bal 31 restriction nuclease. The DNA fragment was deposited on mica and imaged in buffer using the tapping mode. (Image by Guthold, from ref. 6.) FIGURE 5

microscopes, the imaging process is linear—that is, the image of two point particles is the sum of the images of each particle separately. Consequently, image processing and analysis for such microscopes are based on general linear methods such as Fourier transforms and linear convolutions. In scanning force microscopy the imaging process is fundamentally nonlinear. For example, as illustrated in box 1, the SFM image of two spikes is not the sum of the two individual images, but is the union of two sets (in this case the inverted tip surfaces) corresponding to each spike. Therefore, the methods used for lens-based microscopes are of limited application.

Recently, nonlinear methods of image reconstruction in scanning force microscopy have been developed. The basic imaging process is described as the sliding of one geometric surface (the tip) over another (the sample), assuming no sample compression.[6,14] Generalizations of this approach for noncontact imaging also exist.[15] It is possible to treat these purely geometric effects with a simple algorithm: The sample is thought of as a series of closely spaced, infinitely sharp spikes. During scanning, each spike is imaged as an inverted tip that appears to hang upside-down on the spike. (See the figure in box 1.) The image of the entire object is the union of this set of inverted tips. At points where sample features are shallow and blunt (compared to the tip), the image closely resembles the true surface. But at steep features, crevices and interior corners, the image differs significantly. Usually sharp spatial features appear to be broadened.

Figure 6 shows an example of image reconstruction involving chicken erythrocyte chromatin fibers.[16] The high, round features are nucleosomes, each connected to adjacent ones by a segment of a double-stranded DNA molecule. A model of one of these fibers (figure 6a) and its calculated images (figures 6b and 6c), match the experimental image (figure 6d) qualitatively. Such comparisons between real and model images are helpful for interpreting SFM images in terms of the underlying molecular structure.

Future work

The rapid technical developments in scanning force microscopy and their application to biology suggest that this technique may indeed fill the gap between optical and electron microscopes. The unique capabilities of the SFM to operate at high resolution in liquids could make a range of complex macromolecular assemblies whose complexity currently places them outside the realm of x-ray crystallography and nuclear magnetic resonance accessible to study. For that to happen, however, future developments will be necessary along three main lines:

▷ Improved spatial resolution through the use of sharper tips.

▷ Reduced tip–sample forces and, correspondingly, reduced sample damage.

▷ New methods for the controlled attachment of samples to surfaces in liquids.

These developments will all be interdependent. Im-

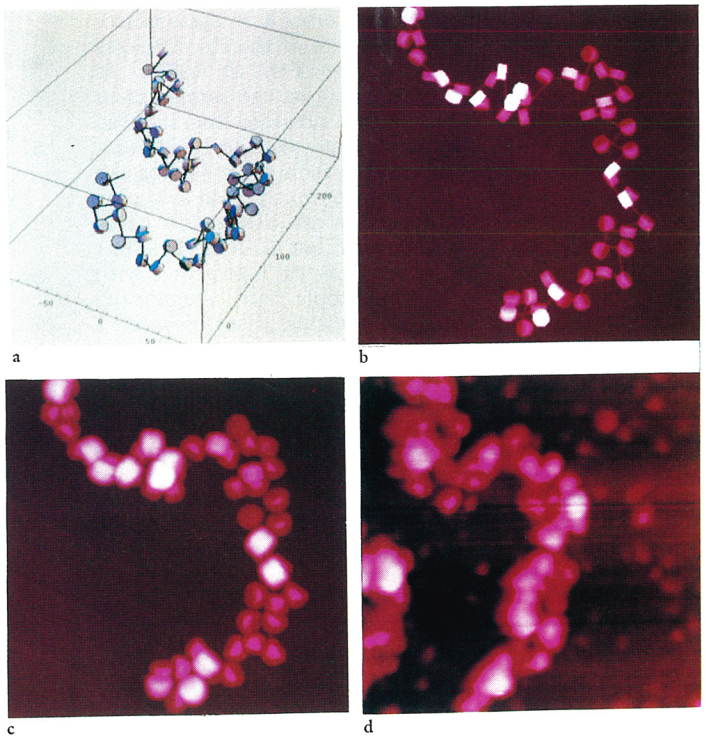

MODEL AND EXPERIMENTAL SFM images of native chromatin fibers. **a:** The structure of a model chromatin fiber in three-dimensional space. The length of the linker DNA varies between 51 and 73 base pairs. The unit of the axes is nanometers. **b:** The model fiber in **a**, after being projected onto a plane, displayed with the SFM image format. **c:** The model fiber in **b** after it was mathematically scanned by and partially compressed by a parabolic tip (with a radius of curvature of 10 nm) to simulate the imaging process in SFM. **d:** Experimental SFM image of a glutaraldehyde-fixed chromatin fiber. The similarity between calculated and experimental images (**c** and **d**, respectively, in this example) helps confirm that the round features correspond to nucleosomes and the thin lines to linker DNA, and that the apparent difference in nucleosome height is a consequence of the fiber's three-dimensionality. (Image and simulation by Guoliang Yang, University of Oregon; from ref. 16.) FIGURE 6

Box 3. Resolution in the noncontact mode

In noncontact scanning force microscopy, spatial resolution depends on both the dimensions of the tip and the distance between tip and sample. It is instructive to consider the best possible situation: the resolution obtained using an infinitely thin tip, or "line tip," to image a point particle using short-ranged attractive van der Waals interactions. In noncontact imaging, the quantity actually measured is the gradient of the force in the direction perpendicular to the sample surface. If the end of the line tip is at a height h above the surface, the gradient of the force at a lateral distance r from the particle is

$$\frac{\partial F(r,h)}{\partial z} = -\left(\frac{\lambda \aleph}{\pi^2 \delta_1 \delta_2 h^7}\right)\frac{6-(r/h)^2}{[(r/h)^2+1]^{9/2}}$$

where δ_1 and δ_2 are the densities of the interacting media (tip and sample); λ is the number of atoms per unit length of the line tip; and $\aleph$ is the Hamaker constant, which depends on the refractive and dielectric properties of the interacting media and the medium surrounding them. Defining the resolution as twice the distance r at which the force of interaction falls to half the maximum, the above expression predicts that the optimal resolution in the noncontact mode is $r = 0.8\,h$.

Thus, with an ideal tip and ideal imaging conditions (no noise and high sensitivity), resolution in the noncontact mode is ultimately limited by the size of the tip–sample gap. A microscope capable of imaging in water with a resolution of 10–20 angstroms would have a major impact on structural studies in biology. It would require that a very sharp tip be scanned at a height of at most 12–24 Å, which is technically challenging but not unrealistic.

Such a microscope would be ideal for soft, easily deformed biological samples. The forces acting in the noncontact mode can be estimated from the van der Waals force between a sphere of radius R_1 (the tip) with a sphere of radius R_2 (a protein molecule) at a distance q. This force is given by[18]

$$F_{\text{noncontact}} = \frac{\aleph y^3(1+2x+y)}{24R_1x^2(1+x)^2(x+y)^2(1+x+y)^2}$$

where $x = q/2R_1$ and $y = R_2/R_1$. Taking $R_1 = 1.5$ nm, $R_2 = 2.5$ nm, $q = 1.5$ nm and $\aleph = 4\times10^{-20}$ J, this expression gives a noncontact force of about 7×10^{-13} N, which is three orders of magnitude smaller than the force in the tapping mode.

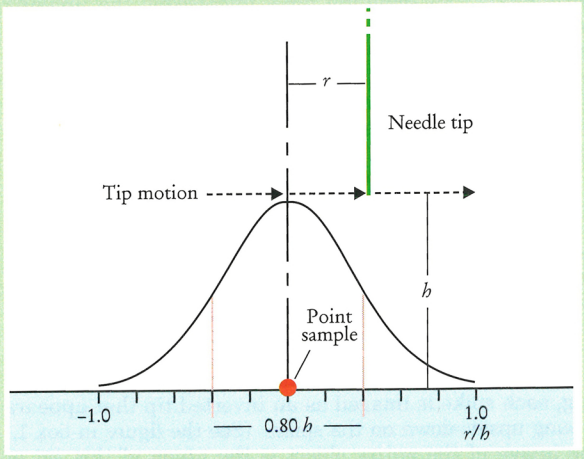

proved spatial resolution using sharper tips requires that tip–sample forces be reduced to preserve both the tip and the sample. Sample damage can increase with tip sharpness because, although attractive forces decrease approximately with the radius of curvature of the tip, the area of contact decreases with the square of the tip radius. As tips get sharper the net force acting on the sample must therefore be reduced to prevent the pressure from increasing. Similarly, when imaging in physiological solutions, tip–sample forces must be smaller than those holding the sample to the substrate to prevent the tip from sweeping the sample off the surface. One solution would be to increase the sample's attachment, but that might affect its native configuration or prevent its interaction with other molecules. Reducing tip–sample forces is again the better solution. Calculations indicate that forces of 1 piconewton or less will preserve the native structure of biological samples.

The above requirements could all be met simultaneously by a noncontact microscope capable of reliable operation in liquids, or by a microscope capable of tapping at very low forces. Moreover, either instrument could use fragile, ultrasharp tips to provide higher spatial resolution on biological samples bound only lightly to the substrate. Either solution will most likely require gaining a sharp cantilever resonance in the viscous liquid environment. The embodiment of such an instrument is perhaps the most important technical challenge for future applications of scanning force microscopy in biology.

References

1. G. Binnig, C. F. Quate, C. Gerber, Phys. Rev. Lett. **56**, 930 (1986).
2. C. Bustamante, D. Keller, G. Yang, Current Opinion Struct. Bio. **3**, 363 (1993).
3. D. Sarid, *Scanning Force Microscopy with Applications to Electric, Magnetic, and Atomic Forces*, Oxford U.P., New York (1991), chap. 13.
4. H. K. Wickramasinghe, J. Vac. Sci. Technol. A**8**, 363 (1990).
5. F. Ohnesorge, G. Binnig, Science **260**, 1451 (1993).
6. C. Bustamante, D. A. Erie, D. Keller, Curr. Opin. Struct. Biol. **4**, 750 (1994).
7. J. Israelachvili, *Intermolecular and Surface Forces with Applications to Colloidal and Biological Systems*, Academic, San Diego, Calif. (1991), chap. 11.
8. D. M. N. Jondle, L. Ambrosio, J. Vesenka, E. Henderson, Chromosome Research **3**, 239 (1995).
9. D. A. Erie, G. Yang, H. Schultz, C. Bustamante, Science **266**, 1562 (1994).
10. F. A. Schabert, A. Engel, Biophys. J. **67**, 2394 (1994).
11. H. G. Hansma, J. H. Ho, Ann. Rev. Biophys. Biomol. Struct. **24**, 115 (1994).
12. M. Guthold, M. Bezanilla, D. A. Erie, B. Jenkins, H. G. Hansma, C. Bustamante, Proc. Natl. Acad. Sci. USA **91 (26)**, 12927 (1994).
13. M. Bezanilla, B. Drake, E. Nudler, M. Kashlev, P. K. Hansma, H. G. Hansma, Biophys. J. **67**, 1 (1994).
14. D. Keller, Surf. Sci. **253**, 353 (1991).
15. G. S. Pingali, R. Jain, *Proc. IEEE Workshop on Applications of Computer Vision*, IEEE Computer Society Press, New York (1992), p. 282.
16. G. Yang, S. Leuba, J. Zlatanova, K. van Holde, C. Bustamante, Nature Structural Biology **1**, 761 (1994).
17. L. D. Landau, E. M. Lifshitz, *Course of Theoretical Physics, Volume 7, Theory of Elasticity*, 3rd ed., Pergamon, Oxford, UK (1986), p. 67.
18. H. C. Hamaker, Physica **4**, 1058 (1937). ■